The Astronomical Journal, 127:3168–3179, 2004 June
© 2004. The American Astronomical Society. All rights reserved. Printed in U.S.A.

EXPLORING NARROW-LINE SEYFERT 1 GALAXIES THROUGH THE PHYSICAL PROPERTIES OF THEIR HOSTS[1]

V. Botte,[2] S. Ciroi,[2] P. Rafanelli, and F. Di Mille
Dipartimento di Astronomia, Università di Padova, vicolo dell'Osservatorio 2, I-35122 Padova, Italy
Received 2003 December 23; accepted 2004 February 25

ABSTRACT

In this work we address the still open question of the nature of narrow-line Seyfert 1 galaxies (NLS1s): are they really active nuclei with lower mass black holes (BHs) than Seyfert 1 galaxies (S1s) and quasars? Our approach is based on the recently discovered physical connections between nuclear supermassive BHs and their hosting spheroids (spiral bulges or elliptical galaxies). In particular, we compare BH masses of NLS1s and S1s, analyzing the properties of their hosts by means of spectroscopic and photometric data in the optical wavelength domain. We find that NLS1s fill the low BH mass and bulge luminosity values of the $M_{\rm BH}$-M_B relation, a result strongly suggesting that NLS1s are active nuclei in which less massive BHs are hosted by less massive bulges. The correlation is good, with a relatively small scatter fitting simultaneously NLS1s, S1s, and quasars. On the other hand, NLS1s seem to share the same stellar velocity dispersion range as S1s in the $M_{\rm BH}$-σ_* relation, indicating that NLS1s have a smaller BH/bulge mass ratio than S1s. These two conflicting results support in any case the idea that NLS1s could be young S1s. Finally, we do not confirm the significantly nonlinear BH-bulge relation claimed by some authors.

Key words: galaxies: active — galaxies: bulges — galaxies: nuclei — galaxies: Seyfert — quasars: general

1. INTRODUCTION

Narrow-line Seyfert 1 galaxies (NLS1s) belong to the family of active galactic nuclei (AGNs) and owe their name to the peculiar properties that distinguish them from other type 1 AGNs. In general a Seyfert 1 (S1) is classified as NLS1 if its nuclear spectrum shows the permitted lines only slightly broader [FWHM(Hβ) < 2000 km s^{-1}] than the forbidden ones (Osterbrock & Pogge 1985). But NLS1 galaxies are also characterized by a strong Fe II emission, a soft X-ray slope steeper than the slope typical of S1 galaxies, rapid and large soft X-ray variability (Boller, Brandt, & Fink 1996), a weak big blue bump in the optical/UV range, likely shifted toward higher energies (Pounds et al. 1987), a bright IR emission, and a nuclear supersolar metallicity (Mathur 2000; Komossa & Mathur 2001).

Even though NLS1s have been known for almost 20 years (Osterbrock & Pogge 1985), their nature is still a matter of debate. For example, at present the reason for the narrowness of broad permitted lines in NLS1s is not clear. Boller et al. (1996) suggested that if the gravitational force of the central black hole (BH) is the main cause of the motion of the broad line region (BLR) clouds, narrower optical emission lines will result from smaller $M_{\rm BH}$ ($\sim 10^6$–10^7 $M_\odot$), provided that the BLR distance from the central source does not change strongly with $M_{\rm BH}$. These BHs with smaller masses are expected to accrete matter at near- or super-Eddington rates in order to maintain the relatively normal observed luminosities. Recently, Mathur et al. (2001) proposed that NLS1s may be relatively young AGNs hosting BHs still in a growing phase. Nevertheless, other authors suggested that if the BLR clouds were largely confined to a plane, as seems to happen in radio-loud AGNs (see, e.g., McLure & Dunlop 2002 and references therein), NLS1 galaxies could be simply a case in which their BLR is observed more face-on than in S1s (see, e.g., Osterbrock & Pogge 1985). Smith et al. (2002) pointed out that a partly obscured BLR could also justify narrow permitted lines, but these last two scenarios should produce polarization. They claimed that Hα polarization properties of the NLS1s are indistinguishable from those of S1s, excluding obscuration of the inner regions of the BLR or a face-on orientation of a disklike BLR as the explanation for the relatively narrow broad-line profiles.

The connection between the physical properties of nuclear supermassive BHs and their host galaxies, on which several works have focused in recent years, might turn out to be a powerful tool to understand the nature of NLS1s and settle the above cited controversies. Kormendy & Richstone (1995) first found a correlation between BH mass ($M_{\rm BH}$) and the absolute B magnitude of the spheroidal component (M_B). Magorrian et al. (1998) determined $M_{\rm BH}$ values for a sample of 32 nearby galaxies and suggested that $M_{\rm BH}$ is proportional to $M_{\rm bulge}$, such that on average $M_{\rm BH}/M_{\rm bulge} \sim 0.005$. Other authors estimated a similar mass ratio, $\sim$0.002 (see, e.g., Ho 1999; Marconi & Hunt 2003). Recently, studying a sample of nearby galaxies Gebhardt et al. (2000a), Ferrarese & Merritt (2000), and Tremaine et al. (2002) have shown that $M_{\rm BH}$ is tightly correlated with the velocity dispersion of the bulge stellar component (σ_*), although they disagreed about the value of the slope.

In AGNs as well, BHs are expected to correlate with their host bulges. This possibility was explored on a sample of PG quasars by Laor (1998), who found agreement with the relation of Magorrian et al. (1998). Wandel (1999) claimed that Seyfert galaxies show on average an $M_{\rm BH}/M_{\rm bulge}$ ratio systematically lower than that of normal galaxies and quasars, a discrepancy recently corrected by means of updated data (Wandel 2002). Gebhardt et al. (2000b) included in their work seven AGNs for which the $M_{\rm BH}$ values were obtained by

[1] Partially based on observations made with the Asiago 1.82 m telescope of the Padova Astronomical Observatory.
[2] Guest Investigator of the UK Astronomy Data Centre.

means of the reverberation mapping technique. They found that these objects were in agreement with their previous $M_{\rm BH}$-σ_* correlation. Further support came from McLure & Dunlop (2001) and from Wu & Han (2001), who studied samples of quasars and Seyfert galaxies and did not find any evidence that Seyfert galaxies follow a different $M_{\rm BH}$-$M_{\rm bulge}$ relation from that of quasars or nearby galaxies.

Until now no agreement has been reached regarding NLS1s. Mathur, Kuraszkiewicz & Czerny (2001) and very recently Bian & Zhao (2004) and Grupe & Mathur (2004) showed that the $M_{\rm BH}/M_{\rm bulge}$ ratio in NLS1s is significantly smaller than that of Seyfert galaxies. Conversely, Wang & Lu (2001), studying a sample of 59 NLS1s observed spectroscopically by Véron-Cetty et al. (2001), found that there is no clear difference in the $M_{\rm BH}$-σ_* relation (where σ_* is represented by the [O III] emission line width) between NLS1s, broad-line AGNs, and nearby galaxies.

Our purpose in this work is to investigate the nature of NLS1s by exploring the physical properties of their bulges, namely the luminosity and the nuclear stellar velocity dispersion. Our approach makes use of both new observational data and data from the literature. The necessary corrections are applied to the latter in order to obtain a data set that is as homogeneous as possible. Furthermore, a main difference with respect to several other works on this topic is that when determining the bulge properties of the host galaxies we take into account the influence of the AGN, which as we show, can be nonnegligible and affect the results considerably. The structure of the paper is as follows: in § 2 we present our data set and derive and compare BH mass values for a sample of NLS1s and S1s. In § 3 we estimate the blue absolute magnitudes and the stellar velocity dispersions of their bulges. Our results are summarized and discussed in § 4.

2. BLACK HOLE PROPERTIES

2.1. *Spectroscopic Data*

First, we have isolated a list of 23 NLS1 and 23 S1 galaxies of the northern hemisphere from Véron-Cetty et al. (2001) on the basis of their "S1n" and "S1.0" classification and of the redshift $z < 0.1$, chosen to avoid having Hβ and [O III] lines fall in a spectral region with strong night-sky emission lines.

No other selection criteria were applied. This sample is complete up to visual magnitude 15.5, corresponding to 80% of the selected galaxies, and it is therefore useful for our purposes.

Out of this sample, we were able to collect optical spectra for 22 NLS1s and 15 S1s. In particular, 19 NLS1s and seven S1s were extracted from the public data available in the Isaac Newton Group (ING) archive. These spectra were obtained for different purposes in 1995, 1996, 1999, and 2000, mostly with the Intermediate Dispersion Spectrograph (IDS) mounted at the 2.5 m Isaac Newton Telescope (INT, Canary Islands, Spain), and the others with the ISIS Double Beam Spectrograph (ISIS) at the 4.2 m William Herschel Telescope (WHT, Canary Islands, Spain). Three other NLS1s and eight S1s were observed directly by us in 2002 September and in 2003 January using the Asiago Faint Object Spectrograph and Camera (AFOSC) mounted at the 1.82 m telescope of the Padova Astronomical Observatory (Asiago, Italy). Tables 1 and 2 summarize the instrumental setup and the total wavelength coverage for each observation.

All spectra were reduced with the same procedure. The usual data reduction steps—bias and flat-field corrections, cosmic-ray removal, wavelength linearization, sky-background subtraction, and flux calibration—were carried out with IRAF packages.[3] A one-dimensional spectrum of the nucleus was obtained for each galaxy summing a number of pixels along the spatial direction on the basis of the seeing conditions. When available, adjacent spectral ranges of the same source were combined. Then a correction for Galactic extinction was applied using for each galaxy the value given by NED[4] and the Cardelli, Clayton, & Mathis (1989) extinction law. The so-processed spectra were shifted to the rest frame, and the intrinsic absorption was removed following the technique used by Crenshaw et al. (2002). In particular, we determined the value of the internal reddening using the relation: $E(B-V) = 2.5\ [\log(X_B) - \log(X_V)]$, where X is the ratio of the fit of the Mrk 478 continuum to that of the other galaxies of the sample evaluated at the effective wavelengths of the B (4400 Å) and V (5500 Å) photometric bands. Contrary to Crenshaw et al. (2002), we could not use Mrk 493 as a reference because its spectrum was available only for wavelengths greater than 4400 Å thus yielding a rather uncertain estimate of X_B. The spectrum of Mrk 478 was used instead, after correction for internal absorption by means of the hydrogen column density $N_{\rm H} = 2.0 \pm 10^{20}$ cm^{-2}, given by Boller et al. (1996).

One of the peculiar features in the optical spectrum of most NLS1 galaxies is the presence of strong emission of Fe II multiplets centered at 4570, 5190, and 5300 Å. In order to remove them and allow a more precise measure of Hβ and [O III] emission lines we produced an Fe II template using the spectrum of the NLS1 I Zw 1 as suggested by Boroson & Green (1992). The template was scaled in intensity and conveniently smoothed to match the spectrum of each galaxy showing evident Fe II multiplets and then subtracted.

2.2. *Wrong Classifications*

A fast inspection of each galaxy spectrum allowed us to isolate four NLS1s, Mrk 1126, Mrk 291, Mrk 957, and HB 1557, which in our opinion are wrongly classified. After a multi-Gaussian fit of Hβ, and Hα + [N II] $\lambda\lambda$6548, 6583 emission lines we assert that these active nuclei have permitted lines with a clear composite broad + narrow profile, where the narrow components have widths similar to those of the forbidden lines ($\sim$250–300 km s^{-1}; Fig. 1). This kind of profile is typically shown by intermediate Seyfert galaxies. Indeed, Osterbrock (1989) introduced the notation Seyfert 1.5, 1.8, and 1.9 to indicate the simultaneous presence of narrow and broad permitted lines in many spectra of Seyfert galaxies.

Broad Hβ and Hα components were fitted in Mrk 1126 and Mrk 291, obtaining widths of about 2600–2900 km s^{-1}, while only Hα broad was detected in Mrk 957 and HB 1557, and fitted to widths of about 1600 and 3000 km s^{-1}, respectively. We observe that the value of Hα broad in Mrk 957 is lower than the others. This could be caused by a nonreliable multi-Gaussian fit of Hα + [N II] blend. Indeed we have the impression that a blue [N II] component exists in addition to the others already identified, but the spectral resolution is not sufficiently high to obtain a stable fit of the profile with six or more Gaussians. Moreover, we noted that Mrk 957 is the only

[3] IRAF is written and supported by National Optical Astronomy Observatory (Tucson, Arizona), which is operated by Association of Universities for Research in Astronomy (AURA), Inc., under cooperative agreement with the National Science Foundation.

[4] NASA Extragalactic Database.

TABLE 1
NARROW-LINE SEYFERT 1 OBSERVATION LOG

Name	R.A. (J2000)	Decl. (J2000)	Telescope	Instrument	λ Range (Å)	Date	Exposure Time (s)	$\Delta\lambda$ (Å)
Mrk 335	00 06 19.5	+20 12 10	1.82 m	AFOSC	4000–6500	2002 Sep 09	1800	12
					6000–8100	2002 Sep 09	1200	9
Mrk 957	00 41 53.4	+40 21 18	INT	IDS	4400–6000	1996 Aug 08	1200	2.5
					6000–7600	1996 Aug 10	1200	2.5
I Zw 1	00 53 34.9	+12 41 36	INT	IDS	4400–6000	1996 Aug 08	1800	2.5
					5900–7500	1996 Aug 07	1200	2.5
Mrk 359	01 27 32.5	+19 10 44	INT	IDS	4400–6000	1996 Aug 08	900	2.5
					5900–7500	1996 Aug 08	900	2.5
E0144	01 46 44.8	−00 40 43	INT	IDS	4400–6000	1996 Aug 09	1200	2.5
					5900–7500	1996 Aug 07	1200	2.5
Mrk 1044	02 30 05.4	−08 59 53	INT	IDS	4400–6000	1996 Aug 08	900	2.5
					5900–7500	1996 Aug 06	900	2.5
IR 04312	04 34 41.5	+40 14 22	1.82 m	AFOSC	4000–6500	2002 Sep 10	1800	12
UGC 3478.....	06 32 47.2	+63 40 25	1.82 m	AFOSC	4000–6500	2003 Jan 27	1800	12
					6000–8100	2003 Jan 27	1200	9
Mrk 705	09 26 03.3	+12 44 04	INT	IDS	4400–6000	1995 Jan 17	1500	3.5
Mrk 142	10 25 31.3	+51 40 35	INT	IDS	4400–6000	1995 Jan 17	1800	4
					5850–7800	1995 Jan 17	1800	4
IC 3599	12 37 41.2	+26 42 27	WHT	ISIS	3350–5900	1995 Mar 05	450	9
					5400–8350	1995 Mar 05	450	2.5
Mrk 684	14 31 04.8	+28 17 14	INT	IDS	4200–7400	1996 Aug 11	1200	6.5
Mrk 478	14 42 07.4	+35 26 23	INT	IDS	4100–7200	1996 Aug 10	900	6.5
Mrk 291	15 55 07.9	+19 11 33	INT	IDS	4400–6000	1996 Aug 07	900	2.5
					5900–7500	1996 Aug 05	900	2.5
Mrk 493	15 59 09.6	+35 01 48	INT	IDS	4400–6000	1996 Aug 06	900	2.5
					5900–7500	1996 Aug 08	900	2.5
Hb 1557	15 59 22.2	+27 03 39	INT	IDS	4400–6000	1996 Aug 08	1200	2.5
					5900–7500	1996 Aug 08	1200	2.5
Kaz 163.....	17 46 59.8	+68 36 39	INT	IDS	4400–5950	1996 Aug 07	1200	2.5
					5900–7450	1996 Aug 05	1200	2.5
Mrk 507	17 48 38.4	+68 42 16	INT	IDS	4300–6000	1996 Aug 09	1200	2.5
					5900–7050	1996 Aug 07	900	2.5
Mrk 896	20 46 20.9	−02 48 45	INT	IDS	4400–5950	1996 Aug 08	1200	2.5
					5900–7450	1996 Aug 06	1200	2.5
Ark 564.....	22 42 39.3	+29 43 31	WHT	ISIS	4700–5550	1999 Jun 10	600	1.5
UCM 2257.....	22 59 32.9	+24 55 06	INT	IDS	4250–7450	1996 Aug 11	1800	2.5
Mrk 1126	23 00 47.8	−12 55 07	INT	IDS	4400–6000	1996 Aug 09	1200	6.5
					5900–7500	1996 Aug 07	1200	2.5

NOTE.—Units of right ascension are hours, minutes, and seconds, and units of declination are degrees, arcminutes, and arcseconds.

one out of the four galaxies showing Fe II multiplets, whose strong emission is one of the typical features of NLS1s.

Therefore, we excluded these four galaxies from our NLS1 sample, but we included UGC 3478, which was until now wrongly classified as S1. UGC 3478 has an optical nuclear spectrum typical of NLS1s: we have found narrow Balmer emission lines [FWHM(Hβ) = 1600 km s^{-1}], a low [O III] λ5007/Hβ ratio (=4.8), and a strong emission of [Fe II] multiplets. Moreover, the luminosities of the low-ionization emission lines, [N II] λ6583, [S II] $\lambda\lambda$6716, 6731, and [O I] λ6300, assume weak values. The *ASCA* hard X-ray spectrum, available in the TARTARUS database, shows a steep power-law distribution with photon index $\Gamma_X \sim 2.3$, similar to that given by Leighly (1999) for NLS1s ($\Gamma_X \sim 2.19 \pm 0.10$).

2.3. *BH Mass Estimation*

The stellar dynamical techniques used to derive BH masses are severely limited for AGNs, since they require high signal-to-noise ratio measurements of stellar absorption features that are often lost in the glare of a bright active nucleus (Nelson 2000). The alternative solution consists in applying the virial theorem to the BLR clouds, gravitationally bound to the central mass and located at distances of few light-days (S1s) to several light-weeks (quasars):

$$M_{\rm BH} = R_{\rm BLR} V^2 G^{-1}, \quad (1)$$

where $R_{\rm BLR}$ is the radius of the BLR, V the velocity of the broad-line–emitting gas, and G the gravitational constant. Even if there is no general consensus about the dynamics of the BLR, evidence for Keplerian motions of the BLR clouds was found by Peterson & Wandel (1999) and Wandel, Peterson, & Malkan (1999), using the reverberation mapping technique. This is one of the major tools for studying correlated variations of the lines and continuum emission of AGNs and determining the size ($R_{\rm BLR}$) and the geometry of the BLR (see, e.g., Peterson 1993).

However, the lack of long-term variability monitoring makes it difficult to measure the $R_{\rm BLR}$ of most Seyfert galaxies using this method. As an alternative, the $R_{\rm BLR}$ can be estimated

TABLE 2
SEYFERT 1 OBSERVATION LOG

Name	R.A. (J2000)	Decl. (J2000)	Telescope	Instrument	λ Range (Å)	Date	Exposure Time (s)	$\Delta\lambda$ (Å)
Mrk 1146	00 47 19.4	+14 42 13	1.82 m	AFOSC	4000–6500	2002 Sep 30	1200	7.5
					6000–8100	2002 Sep 30	1200	5.5
UGC 524	00 51 35.0	+29 24 05	1.82 m	AFOSC	4000–6500	2003 Jan 26	1800	12
					6000–8100	2003 Jan 26	1200	9
Mrk 975	01 13 51.0	+13 16 18	1.82 m	AFOSC	4000–6500	2003 Jan 27	1800	12
					6000–8100	2003 Jan 27	1200	9
Mrk 358	01 26 33.6	+31 36 59	1.82 m	AFOSC	4000–6500	2002 Sep 30	1800	7.5
					6000–8100	2002 Sep 30	1200	5.5
Mrk 1040	02 28 14.5	+31 18 42	1.82 m	AFOSC	4000–6500	2002 Sep 30	1200	7.5
					6000–8100	2002 Sep 30	1200	5.5
UGC 3142	04 43 46.8	+28 58 19	1.82 m	AFOSC	6000–8100	2003 Jan 25	1800	12
					6000–8100	2003 Jan 25	1200	9
Mrk 10	07 47 29.1	+60 56 01	INT	IDS	4400–5950	1995 Jan 14	1500	3.5
Mrk 382	07 55 25.3	+39 11 10	1.82 m	AFOSC	4000–6500	2003 Jan 25	1800	12
					6000–8100	2003 Jan 25	1200	9
Mrk 124	09 48 42.6	+50 29 31	INT	IDS	4400–6000	1995 Jan 17	1500	3.5
NGC 3080	09 59 55.8	+13 02 38	INT	IDS	4400–6000	1995 Jan 15	1800	3.5
Mrk 40	11 25 36.2	+54 22 57	INT	IDS	4400–6000	1995 Jan 17	1500	3.5
Mrk 205	12 21 44.0	+75 18 38	1.82 m	AFOSC	4000–6500	2003 Jan 25	1800	12
					6000–8100	2003 Jan 25	1200	9
Ton 730	13 43 56.7	+25 38 48	WHT	ISIS	3500–6000	1999 Mar 23	1200	4.0
					5800–8250	1999 Mar 23	1200	5.5
3C 382	18 35 03.4	+32 41 47	WHT	ISIS	3700–5350	2000 Jul 06	600	2.5
					6000–7400	2000 Jul 06	600	4.5
3C 390.3	18 42 09.0	+79 46 17	INT	IDS	4300–5800	1995 Jan 14	1800	3.5

from the empirical relationship between the BLR size and the luminosity of the continuum at 5100 Å found by Kaspi et al. (2000):

$$R_{\rm BLR} = 32.9^{+2.0}_{-1.9}\left[\frac{\lambda L_\lambda(5100\ \text{Å})}{10^{44}\ \text{ergs s}^{-1}}\right]^{0.700\pm0.033}. \quad (2)$$

Since the BLR consists of photoionized clouds of gas and since the luminosities of NLS1s and S1s are generally comparable (see, e.g., Padovani & Rafanelli 1988; Boller et al. 1996), we applied this relation, whose validity for a few NLS1s was proved by Peterson et al. (2000). Indeed, after having measured λL_λ (5100 Å) for each object of our sample we verified that NLS1s and S1s have similar optical luminosity of continuum [$\log \lambda L_\lambda(5100\ \text{Å}) = 43.51 \pm 0.65$ vs. 43.08 ± 0.45, respectively], as can be seen in Figure 2.[5]

Some authors produced substantial evidence that the broad-line emitting material has a flattened disklike geometry in radio-loud quasars (see, e.g., Vestergaard, Wilkes, & Barthel 2000). Such evidence is less strong for radio-quiet AGNs, even if very recently Strateva et al. (2003) found that a high percentage of AGNs showing double-peaked Balmer lines are radio-quiet. Therefore, we have estimated the parameter V from the emission-line width of Hβ by assuming that the velocity dispersion in the line-emitting gas is isotropic and after having removed the instrumental width:

$$V = (\sqrt{3}/2)\text{FWHM}(\text{H}\beta). \quad (3)$$

The resulting $M_{\rm BH}$ values are listed in Tables 6 and 7. As expected NLS1s have on average BHs with smaller masses than S1s: $\log M_{\rm BH} = 6.65 \pm 0.64$ vs. 7.37 ± 0.62, a result that depends directly on the narrowness of the Balmer emission lines, since nuclear luminosities and therefore BLR radii are quite similar in both samples. Similar considerations can be found in a contemporary paper by Grupe & Mathur (2004).

Of course, such $M_{\rm BH}$ values are characterized by some uncertainties, and we have tried to analyze them. First of all, the uncertainties given in equation (2) produce errors of less than 15% concerning $R_{\rm BLR}$ calculated values. Second, the luminosity of the continuum is affected by flux calibration errors and by intrinsic variability of the sources. About this last point, following the discussion by Wang & Lu (2001), who noticed that the continuum variation is not larger than a factor of 2 for most AGNs, we assumed a 30% error as an upper limit. The spectrophotometry accuracy, evaluated through multiple observations of standard stars, was estimated around 10%–20% for archival data, and 20%–30% for Asiago data. Combining these errors, we obtain a less than 40% error for $R_{\rm BLR}$. The final uncertainty of $M_{\rm BH}$ is likely less than or around 50%, corresponding to $\sim$0.25 dex in logarithmic scale. It should be taken into account that a nonnegligible fraction of optical light may come from the host galaxy, especially in case of low-luminosity AGNs. Since a precise estimate of the host contribution is not straightforward, we decided to neglect it and remain closer to the procedure followed by Kaspi et al. (2000) in obtaining their empirical relation.

3. BULGE PROPERTIES

After having calculated the masses of the BHs hosted by each galaxy of our NLS1 and S1 sample, we investigated the physical properties of their bulges, deriving their blue luminosities and the values of the central stellar velocity dispersion. Then we explored the connection between bulges and nuclear BHs in order to find out where NLS1s are placed with respect to S1s.

[5] Throughout this paper we assume $H_0 = 75$ km s^{-1} Mpc^{-1}.

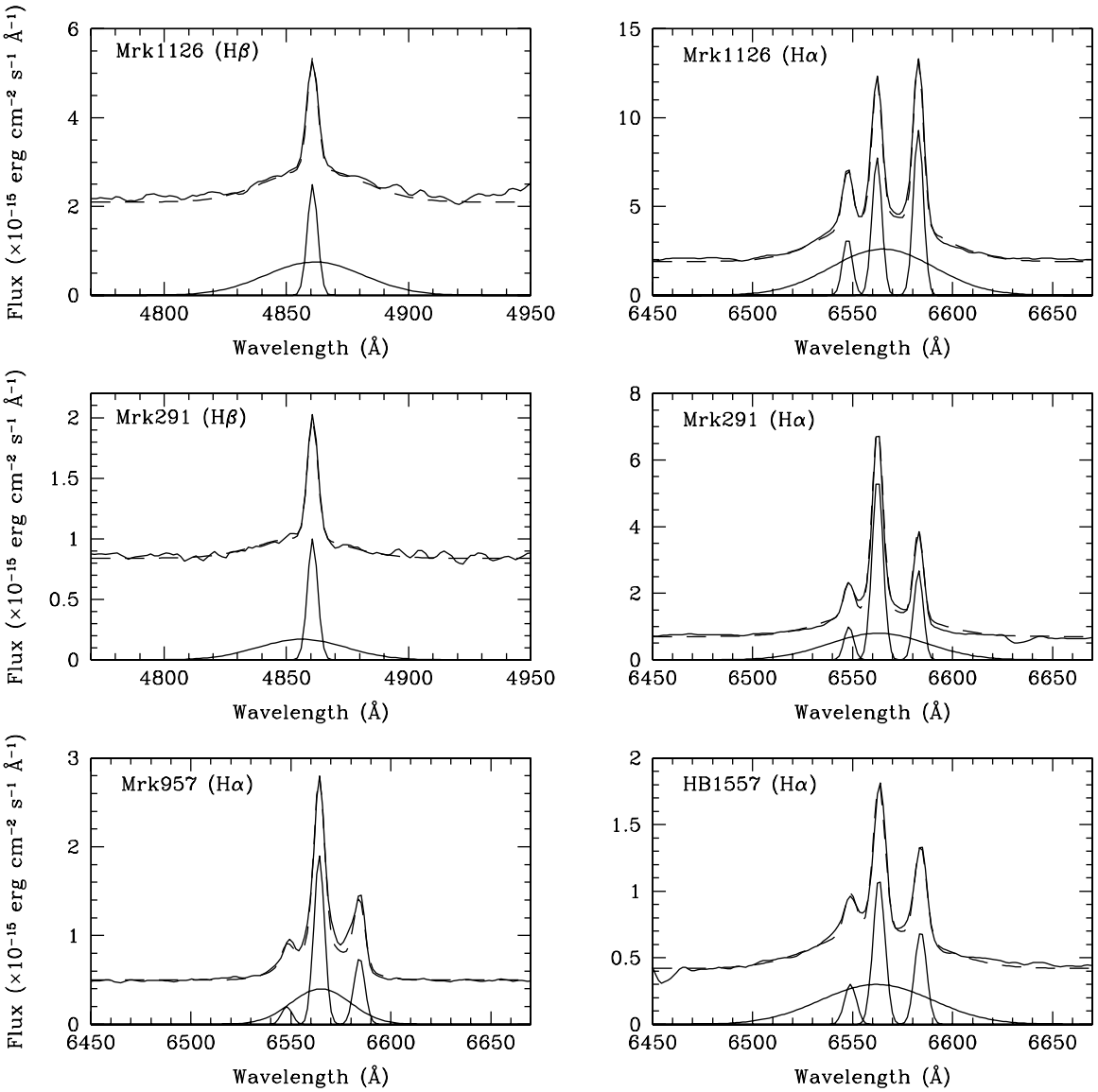

FIG. 1.—Multi-Gaussian deblending of broad and narrow Hβ and Hα emission lines for the wrongly classified NLS1s. In each panel the observed profile (*top*) is compared with the fit (*dashed line*). Single Gaussian components are also shown (*bottom*).

3.1. *Blue Luminosity*

Since we did not have at our disposal photometric data to measure *B*-band magnitudes (m_B), we took from the literature, when available, values for the objects in our samples (Winkler 1997; MacKenty 1990; Granato et al. 1993; Schmitt & Kinney 2000; Prugniel & Heraudeau 1998). When we found multiple estimates we calculated a median value.

The m_B values were corrected for Galactic extinction (Δm_G), using values given by Schlegel, Finkbeiner, & Davis (1998), and internal absorption (Δm_i), following the relation given in the introduction to the Third Reference Catalogue of Bright Galaxies (RC3; de Vaucouleurs et al. 1991): $\Delta m_i = \alpha_T \log(\sec i)$, where $\alpha_T = 1.5 - 0.03(T-5)^2$ for spiral galaxies ($T \geq 0$). Inclination values i were extracted from the HyperLeda database.[6] The k correction was also applied (Δm_k), again by following the method described in RC3.

[6] See http://leda.univ-lyon1.fr.

Contrary to the methods of several other authors, we decided to take into account the emission-line and nonstellar continuum contributions from the AGN to the total magnitude of each galaxy. To do this we followed the approximations of Whittle (1992). In particular we used the equations (2), (3), (4), and (5) in that paper for $F_{c,\mathrm{F}}$ and $F_{c,\mathrm{H}}$, which are the effective continuum fluxes in *B*-band due to the forbidden and Balmer emission lines. Instead, before calculating the nonstellar continuum flux $F_{c,\mathrm{C}}$, we noticed that Whittle (1992) assumed a typical value of $\sim$100 Å as equivalent width of Hβ . Since we have the spectra and the underlying continuum of Hβ is very similar to the already measured continuum at 5100 Å, we could take as approximation $F_{c,\mathrm{C}} \simeq F_\lambda(5100\ \text{Å})$, having adopted a power law with spectral index $\alpha = -1.0$, as was done by Whittle (1992).

The total nonstellar flux $F_c = F_{c,\mathrm{F}} + F_{c,\mathrm{H}} + F_{c,\mathrm{C}}$ gives the required correction Δm_A to be applied to m_B. The final corrected total magnitudes are given by: $m'_B = m_B + \Delta m_A - \Delta m_i - \Delta m_G - \Delta m_k$.

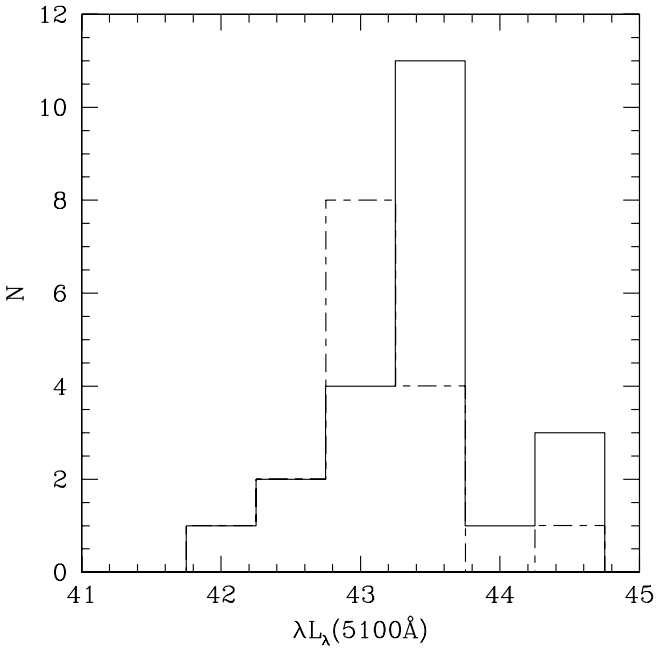

FIG. 2.—Comparison between the distributions of the measured nuclear continuum luminosity for NLS1 (*solid histograms*) and S1 (*dashed histogram*) galaxies. The median values are 43.51 ± 0.65 and 43.08 ± 0.45, respectively.

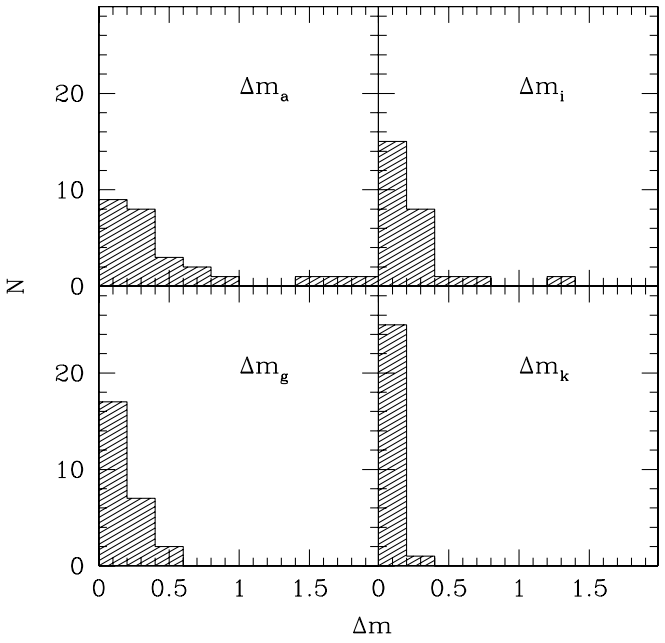

FIG. 3.—Distribution of magnitude correction terms applied to m_B values.

The distribution of these terms is shown in Figure 3. It can be easily noticed that Δm_k plays a minor role in the total contribution to the magnitude corrections, while Δm_A is as important as—and sometimes even more important than—Δm_i and Δm_g. This strongly indicates that neglecting Δm_A can be a dangerous approximation when bright AGNs are considered.

After having converted m'_B into absolute magnitudes M_B, listed in Table 3, we obtained the bulge magnitudes ($M_{B,\mathrm{bulge}} = M_{\mathrm{B}} + \Delta m_{\mathrm{bulge}}$) by applying the formula of Simien & de Vaucouleurs (1986), who found a relation between the bulge-to-total (B/T) luminosity ratio and the morphological type: $\Delta m_{\mathrm{bulge}} = 0.324(T + 5) - 0.054(T + 5)^2 + 0.0047(T + 5)^3$.

The morphology of each galaxy was extracted from the NED and checked by visual inspection of the POSS II digitized images for lower redshift sources, which do not require high spatial resolution, and of the *HST* public images, when available in the archive, for higher redshift galaxies. We excluded the sources for which a "compact" classification was given.

The resulting magnitudes show that NLS1s have typically lower luminosity bulges than S1s: $M_{B,\mathrm{bulge}}(\mathrm{NLS1}) = -18.54 \pm 1.06$ versus $M_{B,\mathrm{bulge}}(\mathrm{S1}) = -19.80 \pm 0.73$.

Giving a realistic estimate of the magnitude errors is not an easy task. All our photometric data are taken from the literature based on CCD observations, with most having an accuracy of less than 0.05 mag. But our M_B values are affected by additional errors, which are introduced by the application of the correction terms: Δm_A, Δm_i, Δm_G, Δm_k, and $\Delta m_{\mathrm{bulge}}$.

Among them, Δm_i and Δm_k are both dependent on the morphological type T, and the error caused by the wrong classification will typically be lower than 0.1 mag. The $\Delta m_{\mathrm{bulge}}$ is also a function of T and increases strongly for late-type spirals. A maximum uncertainty $\Delta T < 2$ in the morphological classification of our objects translates into errors of less than 0.5 and less than 1 mag for early- and late-type spirals, respectively. The Δm_A value is dominated by the contribution of the AGN continuum, since the emission lines affect only $\sim$10% of the total correction. Therefore, Δm_A depends on the spectrophotometric calibration of the continuum and, e.g., an accuracy of 20% will correspond to an uncertainty of $\sim$0.2 mag.

In Figure 4 we plotted $M_{B,\mathrm{bulge}}$ values against M_{BH}. NLS1s and S1s are represented by circles, and triangles, respectively. For completeness, we decided to include in this analysis a sample of 14 quasars (*asterisks*), whose M_{BH} and M_B are given by Kaspi et al. (2000). The sources were selected from their list excluding those having an M_{BH} error greater than the value itself. The absolute magnitudes were corrected for AGN contribution using only the measured continuum flux at 5100 Å, available in the same paper (Table 4). As expected after calculating the median values of the plotted physical quantities, NLS1s fall in the lower ranges of the plot and are well separated from S1s both in BH mass and bulge luminosity values, even if a region of overlap inevitably exists. Moreover, NLS1s, S1s, and quasars seem to be well correlated in the plane M_{BH}-M_B. Therefore, we attempted a least-squares fit (Fig. 4, *solid line*) considering all points together, and obtained

$$M_B = -2.32(\pm 0.18) \log (M_{\mathrm{BH}}) - 3.40(\pm 1.36), \qquad (4)$$

with a correlation coefficient $R = 0.91$.

In order to check the consistency of this result, we first converted blue absolute magnitudes into V band, by applying the morphological type–dependent B–V values given by Jahnke & Wisotzki (2003; their Table 4), and we did a new fit: $M_V = -2.48(\pm 0.19) \log (M_{\mathrm{BH}}) - 3.09(\pm 1.40)$. Then we applied the standard relation, $M_V = +4.83 - 2.5 \log (L_V/L_\odot)$, and a mass-to-luminosity conversion for bulges and spheroidal galaxies found by Magorrian et al. (1998): $\log (M/M_\odot) = -1.11 + 1.18(\pm 0.03) \log (L/L_\odot)$, obtaining as a result

$$\log (M_{\mathrm{BH}}/M_\odot) = 0.85(\pm 0.09) \log (M_{\mathrm{bulge}}/M_\odot) - 2.25(\pm 0.88). \qquad (5)$$

TABLE 3
PHOTOMETRIC DATA OF NLS1 AND S1 GALAXIES

Object	T	m_B	Δm_A	Δm_i	Δm_g	Δm_k	m'_B	M_B	$\Delta m_{\rm bulge}$	$M_{B,\rm bulge}$
Narrow-Line Seyfert 1										
Mrk 335	0	14.20	0.36	0.00	−0.15	−0.12	14.29	−20.80	0.86	−19.94
IZw 1	2	14.47	1.56	−0.17	−0.28	−0.18	15.41	−21.52	1.23	−20.29
Mrk 359	3	14.52	0.67	−0.14	−0.23	−0.04	14.78	−19.34	1.54	−17.80
Mrk 1044	1	14.64	0.39	−0.10	−0.15	−0.06	14.72	−19.30	1.02	−18.28
UGC 3478	5	13.85	0.10	−0.64	−0.39	−0.05	12.87	−20.81	2.54	−18.27
Mrk 142	1	16.06	0.69	−0.14	−0.07	−0.21	16.33	−19.94	1.02	−18.92
Mrk 684	2	15.26	1.73	−0.20	−0.09	−0.14	16.56	−19.77	1.23	−18.54
Mrk 493	4	14.79	0.37	−0.19	−0.11	−0.06	14.80	−20.71	1.97	−18.74
Mrk 896	4	15.15	0.94	−0.37	−0.20	−0.05	15.47	−19.66	1.97	−17.68
Ark 564	4	14.81	1.85	−0.26	−0.26	−0.04	16.10	−18.85	1.97	−16.88
Mrk 590	1	14.45	0.04	−0.05	−0.16	−0.10	14.18	−20.94	1.02	−19.92
Seyfert 1										
Mrk 1146	2	15.53	0.25	−0.23	−0.43	−0.12	15.00	−20.97	1.23	−19.74
UGC 524	3	14.40	0.25	−0.05	−0.27	−0.09	14.24	−21.57	1.54	−20.02
Mrk 975	1	15.67	0.26	−0.26	−0.11	−0.11	15.45	−21.02	1.02	−20.01
Mrk 358	4	14.83	0.09	−0.19	−0.21	−0.09	14.43	−21.84	1.97	−19.87
Mrk 1040	4	13.89	0.20	−1.32	−0.41	−0.03	12.33	−21.77	1.97	−19.80
Mrk 10	4	14.53	0.18	−0.63	−0.20	−0.06	13.82	−21.52	1.97	−19.55
Mrk 382	3	15.30	0.24	−0.06	−0.21	−0.06	15.18	−20.44	1.97	−18.47
Mrk 124	3	15.94	0.53	−0.24	−0.06	−0.13	16.04	−20.73	1.54	−19.19
NGC 3080	1	15.70	0.40	−0.03	−0.13	−0.13	15.82	−19.95	1.02	−18.93
Mrk 205	1	15.23	0.20	−0.25	−0.18	−0.26	14.74	−22.51	1.02	−21.49
Mrk 817	1	14.33	0.46	0.00	−0.03	−0.12	14.64	−20.85	1.02	−19.83
NGC 3516	0	12.59	0.15	−0.08	−0.18	−0.04	12.44	−20.29	0.86	−19.43

NOTES.—Col. (1): Object name; col. (2): morphological type; col. (3): total apparent B magnitude; cols. (4–7): magnitude corrections for col. (4): nuclear nonstellar continuum and emission lines (Δm_A), col. (5): inclination (Δm_i), col. (6): Galactic absorption (Δm_g), and col. (7): redshift (Δm_k); col. (8): total corrected apparent B magnitude; col. (9): total corrected absolute B magnitude; col. (10): correction to obtain bulge magnitude; col. (11): bulge absolute B magnitude.

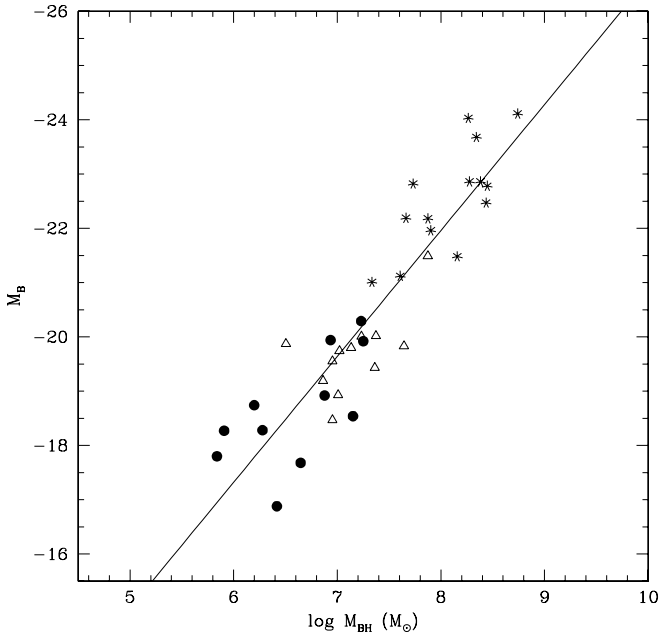

FIG. 4.—$M_{\rm BH}$-M_B relation showing NLS1s (*circles*), S1s (*triangles*), and quasars (*asterisks*). The solid line represents a least-squares fit of the total sample of objects: $M_B = -2.32(\pm 0.18)\log(M_{\rm BH}) - 3.40(\pm 1.36)$. The correlation coefficient is $R = 0.91$.

In Table 5 we compare our results with similar $M_{\rm BH} \propto M^{\alpha}_{\rm bulge}$ relations investigated by other authors. We notice that Wandel (2002) and McLure & Dunlop (2002) obtained slopes of 0.74 and 0.88, respectively, which are consistent with our 0.85 ± 0.09 value.

On the contrary, Bian & Zhao (2003) found a steeper relation ($\alpha = 1.61 \pm 0.59$) for a sample of 22 narrow-line AGNs. The lower number of points and the limited range of the bulge mass values in comparison with their scatter could be the cause of this result. Indeed, the slope of their relation shows an error significantly larger than those presented by other authors. A more stable and less uncertain fit can be obtained by also considering broad-line AGNs, therefore spanning a wider range in both physical quantities, BH and bulge mass. Laor (2001) also found a steeper relation (1.36 ± 0.15). A possible explanation could be that the Kaspi et al. (2000) relation is defined by using monochromatic luminosity, while Laor (1998, 2001) started from bolometric luminosity and applied a constant to convert into L_λ(5100 Å).

3.2. *Stellar Velocity Dispersion*

Contrary to the case of most S1 galaxies (Nelson & Whittle 1995), measuring σ_* in NLS1s with optical spectra is very difficult and sometimes even impossible because of the presence of large and bright Fe II multiplets, which completely suppress the typically used stellar absorption lines, e.g., [Mg I] λ5175 and Fe I λ5269 (Fig. 5). Moreover, NLS1s having bright Fe II often show the Ca II triplet ($\lambda \sim 8550$ Å) in

TABLE 4
QUASAR SAMPLE

Name	R.A. (J2000)	Decl. (J2000)	z	f_λ(5100 Å) (ergs cm^{-2} s^{-1} Å^{-1})	M_B	log L_{1415} (W Hz^{-1})	$M_{\rm BH}$ (10^7 $M_\odot$)	log σ_* (km s^{-1})
PG 0026.....	00 29 13.6	+13 16 03	0.142	2.7×10^{-15}	−22.82	23.71	$5.4^{+1.0}_{-1.1}$	...
PG 0052.....	00 54 52.1	+25 25 38	0.155	2.1×10^{-15}	−23.68	22.95	$22.0^{+6.3}_{-5.3}$	...
PG 0804.....	08 10 58.6	+76 02 42	0.100	5.5×10^{-15}	−22.86	22.64	$18.9^{+1.9}_{-1.7}$	...
PG 0844.....	08 47 42.4	+34 45 04	0.064	3.7×10^{-15}	−21.01	21.79	$2.16^{+0.90}_{-0.83}$	2.356
PG 0953.....	09 56 52.4	+41 15 22	0.239	1.6×10^{-15}	−24.03	23.77	$18.4^{+2.8}_{-3.4}$	...
PG 1211.....	12 14 17.7	+14 03 13	0.085	5.7×10^{-15}	−21.12	22.47	$4.05^{+0.96}_{-1.21}$	2.242
PG 1226.....	12 29 06.7	+02 03 09	0.158	21.3×10^{-15}	−24.11	27.67	$55.1^{+8.9}_{-7.9}$	...
PG 1229.....	12 32 03.6	+20 09 29	0.064	2.1×10^{-15}	−22.18	22.12	$7.5^{+3.6}_{-3.5}$	2.144
PG 1307.....	13 09 47.0	+08 19 49	0.155	1.8×10^{-15}	−22.78	22.63	28^{+11}_{-18}	...
PG 1351.....	13 53 15.8	+63 45 45	0.087	5.1×10^{-15}	−22.19	22.29	$4.6^{+3.2}_{-1.9}$	2.361
PG 1411.....	14 13 48.3	+44 00 14	0.089	3.7×10^{-15}	−21.96	22.38	$8.0^{+3.0}_{-2.9}$	2.432
PG 1613.....	16 13 57.2	+65 43 10	0.129	3.5×10^{-15}	−22.86	23.41	$24.1^{+12.5}_{-8.9}$	...
PG 1617.....	16 20 11.3	+17 24 28	0.114	1.4×10^{-15}	−22.47	22.85	$27.3^{+8.3}_{-9.7}$	...
PG 2130.....	21 32 27.8	+10 08 19	0.061	4.8×10^{-15}	−21.48	22.56	$14.4^{+5.1}_{-1.7}$	...

NOTES.—Col. (1): Object name; cols. (2) and (3): right ascension and declination; col. (4): redshift; col. (5): continumm flux at ~5100 Å; col. (6): absolute B magnitude; col. (7): logarithmic radio luminosity at 1415 MHz (Nelson 2000); col. (8): estimated black hole mass; col. (9): logarithmic stellar velocity dispersion obtained from FWHM([O III]) values by Nelson 2000.

emission (Persson 1988), preventing the use of these lines, which are generally seen in absorption in S1 galaxies.

As an alternative Nelson & Whittle (1996) have shown that the width of the narrow emission line [O III] λ5007 can replace σ_*, expressed in terms of FWHM([O III] λ5007)/2.35, although the correlation between these two quantities is moderately strong with considerable scatter.

Assuming that [O III] λ5007 profiles are dominated by virial motion in the bulge potential, these authors investigated some possible secondary influences on NLR kinematics. For example, they noticed that Seyfert galaxies with high radio luminosity tend to have [O III] λ5007 widths broader than what was expected from gravitational motion because the gas kinematics can be influenced by the presence of a radio jet. They also stressed a slight tendency for barred and/or disturbed Seyfert galaxies to have broader [O III] λ5007 emission lines. Indeed, Barnes & Hernquist (1991) pointed out that the distribution and kinematics of near-nuclear gas can be altered during galaxy interactions.

Since σ_* measurements are available in the literature for only a few of the Seyfert galaxies of our sample, we choose to use FWHM([O III] λ5007) for the others. Then for each object we collected the values of their radio luminosity ($L_{\rm radio}$), taking them from the FIRST survey catalog and the NED, or when no direct measurements were available, using a relationship between the radio luminosity at 1.49 GHz and the $L_{\rm FIR}$ found by Malumyan & Panajyan (2000) for a sample of Seyfert galaxies: $(L_{\rm radio}) = 0.95(\pm 0.06) \log (L_{\rm FIR}) - 12.84(\pm 2.07)$. We calculated $L_{\rm FIR}$ using the fluxes at 60 and 100 μm extracted from the *IRAS* Point Source and Faint Source Catalogues. The total flux $S_{\rm FIR}$ (40–120 μm) was computed by means of the relation (Helou, Soifer, & Rowan-Robinson 1985) $S_{\rm FIR} = 1.26 \times 10^{-14}(2.58 S_{60} + S_{100})$ W m^{-2}, where S_{60} and S_{100} are the flux densities given in Janskys. The so-obtained radio luminosities are listed in Tables 6 and 7. The logarithmic values of σ_* and $M_{\rm BH}$ are plotted in Figure 6, from which we excluded those objects with $L_{\rm radio} > 10^{22.5}$ W Hz^{-1}, as suggested by Nelson & Whittle (1996). NLS1 and S1s are represented by circles and triangles, respectively. In addition, we included quasars from Kaspi et al. (2000; *asterisks*) and nearby nonactive galaxies (*stars*) from Gebhardt et al. (2000a).

A least-squares fit of these values (Fig. 6, *solid line*) gave the relation

$$\log (M_{\rm BH}) = 3.70(\pm 0.37) \log (\sigma) - 0.68(\pm 0.80), \quad (6)$$

with a correlation coefficient $R = 0.81$.

This result is in agreement with Nelson (2000) and Wang & Lu (2001), who found $M_{\rm BH} \propto \sigma_*^{3.70}$, and with Gebhardt et al. (2000a), who found $M_{\rm BH} \propto \sigma_*^{3.75}$ (Fig. 6, *dotted line*). The Merritt & Ferrarese (2001) and Tremaine et al. (2002) relations are also plotted in Figure 6 for comparison (*dashed and dot-dashed lines, respectively*).

TABLE 5
$M_{\rm BH} \propto M_{\rm BULGE}^{\alpha}$ FOR DIFFERENT AUTHORS

Reference	Sample	N	α	R
This work.....	NLS1s, S1s, and quasars	37	0.85 ± 0.09	0.91
Bian & Zhao 2003.....	NL AGNs	22	1.61 ± 0.59	0.74
Wandel 2002.....	AGNs	47	0.74 ± 0.11	0.67
McLure & Dunlop 2002.....	AGNs	72	0.88 ± 0.06	0.77
Laor 2001.....	Quasars and Seyfert	24	1.36 ± 0.21	0.80
Laor 2001.....	AGNs plus quiescent galaxies	40	1.54 ± 0.15	0.80

NOTES.—Col. (1): Bibliographic reference; col. (2): sample; col. (3): number of objects; col. (4): exponent of $M_{BH} \propto M_{\rm bulge}^{\alpha}$ relation; col. (5): correlation coefficient.

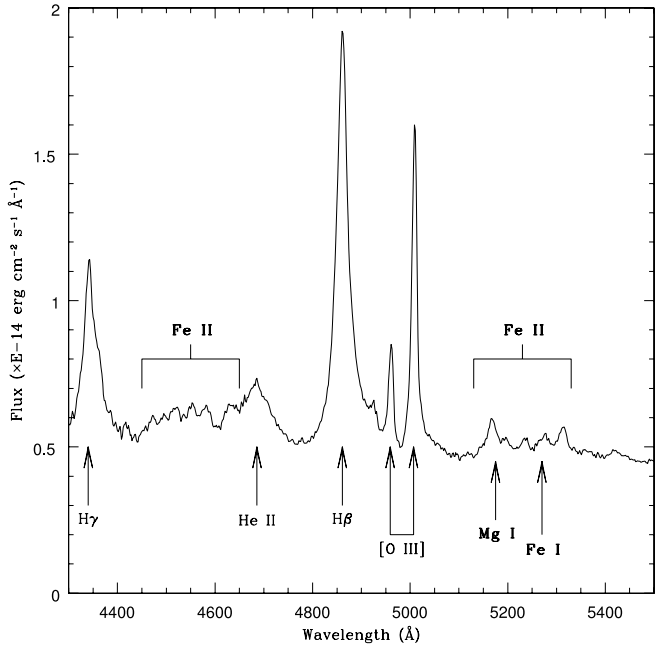

FIG. 5.—Nuclear spectrum of Mrk 335 showing strong Fe II multiplets. Arrows indicate emission lines and the position of stellar absorption (Mg I and Fe I).

We notice a larger scatter in our relation with respect to Gebhardt et al. (2000a). This is mostly caused by the stellar velocity dispersions of NLS1 galaxies, whose values span a range similar to that of S1s. Contrary to what we found in § 3.1, this suggests that NLS1 and S1 galaxies are separated if their BH masses are considered, but are identical in their bulge properties. Moreover, all NLS1s remain below the fit, with some of them closer to the line and, therefore, showing lower stellar velocity dispersions corresponding to lower BH masses, while other NLS1s have clearly larger σ_* than expected. This is likely the reason for having a zero point that is lower than the value obtained by Gebhardt et al. (2000a). A similar result was already obtained by Mathur et al. (2001) and very recently by Bian & Zhao (2004), who used a large sample of low-redshift NLS1s extracted from the Sloan Digital Sky Survey, and by Grupe & Mathur (2004), who used a sample of NLS1s extracted from the *ROSAT* All-Sky Survey. Both found that NLS1s mostly deviate from the $M_{\rm BH}$-σ_* relation defined by Tremaine et al. (2002), showing σ_*-values higher than expected.

A possible reason for this scatter is a spectral resolution that is not sufficient to measure, with high precision, the low σ_*-values predicted by the fit. This objection is well discussed and rejected by Grupe & Mathur (2004). Moreover, in our case, those targets observed at higher resolution are just NLS1s, while S1s, even if observed at lower resolution, show a similar range of σ_* values. Another reason could be that the FWHM ([O III]) – σ_* correlation is not tight and never proved to be valid for NLS1s. Therefore, it is clear that to give a definitive answer, the stellar kinematics in NLS1s should be more carefully investigated by direct measurements of σ_*.

Combining equation (6) with $M_{\rm bulge} \propto \sigma_*^{3.3}$ given by Wang, Biermann, & Wandel (2000 and references therein), who assumed virial equilibrium and $M \propto L^{5/4}$ and $R \propto L^{1/2}$ dependencies, we obtain $M_{\rm BH} \propto M_{\rm bulge}^{1.12\pm0.11}$, which is consistent with $M_{\rm BH} \propto M_{\rm bulge}^{0.85\pm0.09}$ given in § 3.1.

Moreover, starting from equation (6) and converting the BH mass into luminosity by means of the equation $M_V - \log(M_{\rm BH})$ given in § 3.1, and the standard relation $M_V = +4.83 - 2.5\log(L_V/L_\odot)$, we obtain $L \propto \sigma_*^{3.67}$. This is

TABLE 6

NARROW-LINE SEYFERT 1 BLACK HOLE MASSES AND STELLAR VELOCITY DISPERSIONS

NLS1	z	λL_λ(5100 Å) (ergs s^{-1})	$R_{\rm BLR}$ (lt-days)	FWHM (Hβ) (km s^{-1})	$M_{\rm BH}$ ($10^6\ M_\odot$)	log $L_{\rm radio}$ (W Hz^{-1})	log σ_* (km s^{-1})
Mrk 335	0.0260	3.1 10^{43}	14.7 ± 2.4	2007.7	8.61 ± 0.84	21.99[a]	2.140
I Zw 1	0.0606	29.2 10^{43}	69.9 ± 6.6	1439.2	17.00 ± 5.06	22.79[a]	2.769
Mrk 359	0.0167	1.1 10^{43}	7.1 ± 0.9	816.2	0.69 ± 0.09	21.45[a]	1.825
E0144.....	0.0827	2.5 10^{43}	12.6 ± 1.3	1566.2	4.50 ± 0.47	22.75[b]	2.132
Mrk 1044	0.0159	0.6 10^{43}	4.6 ± 0.7	1684.6	1.90 ± 0.29	21.09[b]	2.371
IR 04312	0.0201	3.25 10^{43}	15.0 ± 1.4	1373.7	0.83 ± 0.08	22.14[a]	2.101
UGC 3478.....	0.0131	0.3 10^{43}	2.6 ± 0.4	1460.8	0.81 ± 0.10	21.62[a]	1.996
Mrk 705	0.0287	29.2 10^{43}	68.3 ± 6.3	2153.5	46.13 ± 4.31	22.13[b]	2.281
Mrk 142	0.0448	3.3 10^{43}	15.2 ± 1.4	1876.3	7.54 ± 0.72	21.36[b]	2.200
IC 3599	0.0224	0.1 10^{43}	1.7 ± 0.3	692.9	0.13 ± 0.02	...	2.055
Mrk 684	0.0463	8.7 10^{43}	9.8 ± 1.9	1805.6	14.17 ± 0.91	22.52[c]	2.669
Mrk 478	0.0774	28.9 10^{43}	69.4 ± 6.5	1979.2	30.60 ± 3.34	22.58[b]	2.786
Mrk 493	0.0316	2.1 10^{43}	11.1 ± 1.2	989.9	1.58 ± 0.02	21.81[b]	2.377
Kaz 163.....	0.0637	3.3 10^{43}	15.3 ± 1.5	1844.8	8.76 ± 0.83	22.80[c]	2.332
Mrk 507	0.0553	3.2 10^{43}	15.0 ± 1.4	1876.3	9.44 ± 1.04	22.52[c]	2.519
Mrk 896	0.0265	2.0 10^{43}	10.6 ± 1.1	1673.4	4.43 ± 0.48	21.47[c]	2.153
Ark 564.....	0.0244	4.2 10^{43}	17.9 ± 1.6	971.6	2.61 ± 0.26	22.00[c]	2.026
UCM 2257.....	0.0336	1.6 10^{43}	9.2 ± 1.1	1375.3	2.53 ± 0.30	22.47[c]	2.243
NGC 4051.....	0.0023	...	...	...	1.30 ± 0.10[d]	20.29[b]	1.90[e]
Mrk 590	0.0264	...	...	...	17.8 ± 0.38[d]	22.12[b]	2.23[e]

NOTES.—Col. (1) Object name; col. (2): redshift; col. (3): continuum luminosity at 5100 Å; col. (4): the estimated size of BLR; col. (5): Hβ line width; col. (6): the estimated black hole mass; col. (7): the logarithmic value of stellar velocity dispersion measured from FWHM([O II] λ5007).

[a] $L_{\rm radio}$ from NED.

[b] $L_{\rm radio}$ from the FIRST catalog.

[c] $L_{\rm radio}$ derived from $L_{\rm FIR}$.

[d] Black hole masses from Wu & Han 2001.

[e] Stellar velocity dispersions from Wandel 2002.

TABLE 7
SEYFERT 1 BLACK HOLE MASSES AND STELLAR VELOCITY DISPERSIONS

S1	z	λL_λ(5100 Å) (ergs s^{-1})	$R_{\rm BLR}$ (lt-days)	FWHM(Hβ) (km s^{-1})	$M_{\rm BH}$ (10^7 $M_\odot$)	log $L_{\rm radio}$ (W Hz^{-1})	log σ_* (km s^{-1})
Mrk 1146	0.0391	1.1 10^{43}	7.2 ± 0.9	3141.6	1.05 ± 1.35	21.70[a]	2.363
UGC 524.....	0.0366	1.6 10^{43}	9.3 ± 1.1	4160.6	2.36 ± 0.34	22.62[a]	2.350
Mrk 975	0.0492	1.4 10^{43}	8.3 ± 1.0	3775.4	1.71 ± 0.24	22.75[a]	2.577
Mrk 358	0.0452	0.7 10^{43}	5.2 ± 0.7	2234.8	0.32 ± 0.05	22.32[c]	1.836
Mrk 1040	0.0164	0.8 10^{43}	5.7 ± 0.8	4220.1	1.36 ± 0.20	21.90[a]	2.110
UGC 3142.....	0.0218	1.0 10^{43}	6.6 ± 1.7	10488.5	8.91 ± 0.22	22.36[a]	2.350
Mrk 10	0.0293	1.2 10^{43}	7.5 ± 0.9	3046.9	0.90 ± 0.12	22.27[c]	2.114
Mrk 382	0.0332	1.2 10^{43}	7.4 ± 0.9	2903.3	0.90 ± 0.07	21.86[c]	2.199
Mrk 124	0.0564	3.0 10^{43}	14.1 ± 1.3	1982.3	0.73 ± 0.02	22.55[b]	2.411
NGC 3080.....	0.0355	1.1 10^{43}	6.9 ± 0.9	3172.4	1.02 ± 1.03	22.06[c]	2.334
Mrk 40	0.0206	0.3 10^{43}	3.5 ± 0.8	4042.3	0.93 ± 0.13	21.10[b]	1.965
Mrk 205	0.0703	4.9 10^{43}	19.9 ± 1.7	5082.9	7.48 ± 0.31	22.67[c]	2.275
Ton 730.....	0.0853	2.4 10^{43}	11.8 ± 1.6	3761.6	2.43 ± 0.17	22.78[c]	2.233
3C 390.3	0.0559	5.5 10^{43}	21.8 ± 1.6	5284.7	22.3 ± 2.4	25.82[a]	2.336
3C 382	0.0559	23.6 10^{43}	60.3 ± 5.3	15991.4	224.60 ± 16.31	25.49[a]	2.616
Mrk 79	0.0222	...	...	...	5.20 ± 2.40[d]	22.15[b]	2.10[e]
3C 120	0.0330	...	...	...	3.00 ± 1.30[d]	...	2.21[e]
Mrk 817	0.0314	...	...	...	4.40 ± 1.20[d]	22.24[b]	2.15[e]
NGC 3227.....	0.0038	...	...	...	3.90 ± 3.00[d]	21.36[b]	2.11[e]
NGC 3516.....	0.0088	...	...	...	2.30 ± 0.90[d]	...	2.09[e]
NGC 5548.....	0.0171	...	...	...	12.30 ± 1.60[d]	22.14[b]	2.24[e]
NGC 4151.....	0.0033	...	...	...	1.53 ± 0.93[d]	21.84[b]	1.95[e]

NOTES.—Col. (1) Object name; col. (2): redshift; col. (3): continuum luminosity at 5100 Å; col. (4): the estimated size of BLR; col. (5): Hβ line width; col. (6): the estimated black hole mass; col. (7): the logarithmic value of stellar velocity dispersion measured from FWHM([O III] λ5007).
[a] $L_{\rm radio}$ from NED.
[b] $L_{\rm radio}$ from the FIRST catalog.
[c] $L_{\rm radio}$ derived from $L_{\rm FIR}$.
[d] Black hole masses from Wu & Han 2001.
[e] Stellar velocity dispersions from Wandel 2002.

perfectly in agreement with the Faber–Jackson relation, $L \propto \sigma_*^n$, where $n \sim 3-4$, which is important not only in terms of a distance indicator for elliptical galaxies, but also in studying the physical properties of bulges, as mentioned by Nelson & Whittle (1996).

4. SUMMARY AND CONCLUSIONS

In this work we investigate the nature of NLS1s by an indirect method, that is by using the host galaxy properties to compare black hole masses in NLS1s, S1s, and also quasars.

Starting from the assumption that the emission line clouds of BLR are gravitationally bound to the BH and in random motion, we calculated BH masses of NLS1s obtaining a typical logarithmic value of 6.65 ± 0.64 $M_\odot$, which is almost 1 order of magnitude lower than the value obtained for S1s (7.37 ± 0.62 $M_\odot$). Simultaneously we have confirmed that NLS1s and S1s have quite similar nuclear luminosities: (in logarithm), 43.51 ± 0.65 and 43.08 ± 0.45 $L_\odot$, respectively.

The physical properties of the bulges were investigated in NLS1s and S1s by means of photometric and spectroscopic data. Published total apparent B magnitudes were corrected for extinction, inclination, redshift, and AGN contribution, and converted into absolute magnitudes. Then the bulge magnitudes were calculated taking advantage of the empirical B/T-morphology relation given by Simien & de Vaucouleurs (1986) and used by several authors. We plotted these values against BH masses for NLS1s and S1s, adding quasars extracted from the literature, and we found that NLS1s are mostly confined to the lower ranges of the $M_{\rm BH}$-M_B plane. This result suggests that NLS1s are characterized by less massive BHs hosted in

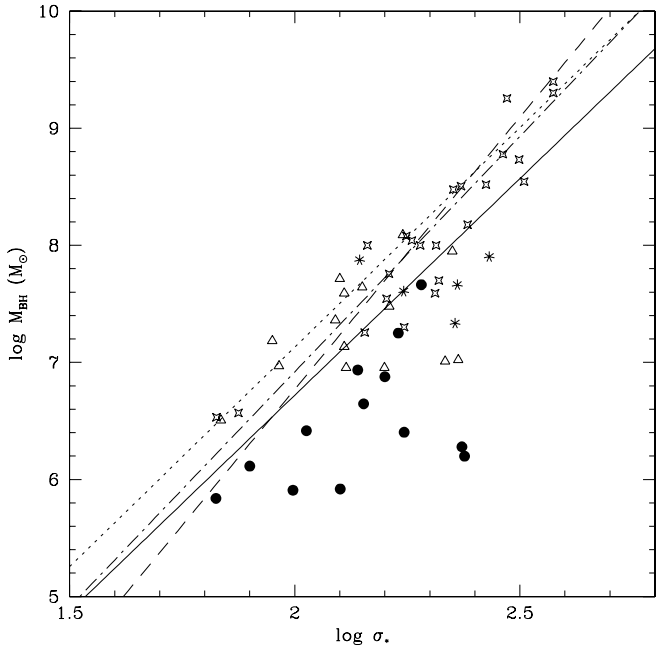

FIG. 6.—$M_{\rm BH}$-σ_* relation, where σ_* is intended in terms of FWHM([O III] λ5007) in all objects for which it was not available in the literature. Symbols are as in Fig. 4, except for open stars, which indicate nearby nonactive galaxies. The solid line is a least-squares fit of the total sample of objects: $\log(M_{\rm BH}) = 3.70(\pm 0.37)\log(\sigma) - 0.68(\pm 0.80)$. The correlation coefficient is $R = 0.81$. The relations found by Gebhardt et al. (2000a; *dotted line*), Merritt & Ferrarese (2001; *dashed line*), and Tremaine et al. (2002; *dot-dashed line*) are also plotted for comparison.

less massive bulges than S1s. This is in agreement with previous findings of Wang & Lu (2001), who explored only the $M_{\rm BH}$-σ_* relation, and in contrast with Mathur et al. (2001) and Bian & Zhao (2003), who claimed NLS1s have lower $M_{\rm BH}/M_{\rm bulge}$ ratios. It is not straightforward to justify the different results found by these authors. After a careful inspection of the effects introduced by each correction that we applied to the photometric data of our targets, we observed that the slightly different way we calculated the correction terms for the AGN contribution and galaxy inclination seems to cause changes that roughly compensate each other. Therefore, we guess that the main source of disagreement is the morphological classification, which strongly affects the resulting bulge magnitudes by quantities in the range of 0.25-0.5 dex for uncertainties discussed in § 3.1.

A fit of NLS1, S1, and quasar values together shows a strongly correlated relation, $M_B = -2.32(\pm 0.18)\log(M_{\rm BH}) - 3.40(\pm 1.36)$, which leads to $M_{\rm BH} \propto M_{\rm bulge}^{0.85\pm0.09}$. Since the slope is close to unity, we do not confirm the results of Laor (2001) and Bian & Zhao (2003), who found a significantly nonlinear BH-bulge correlation.

The velocity dispersion of the bulge stellar component was also explored to check whether NLS1s also have σ_*-values typically lower than those measured in S1s. Since few values of σ_* were available in the literature, we had to calculate the others by measuring the [O III] emission-line widths, and assuming that the gas kinematics is dominated by the bulge potential. As before, we plotted these values against BH masses, adding quasars and also nearby nonactive galaxies, and obtained a good correlation, $M_{\rm BH} \propto \sigma_*^{3.70\pm0.37}$. Contrary to the previous result, NLS1s are not clearly separated from S1s in the $M_{\rm BH}$-σ_* plane. In particular they span similar ranges of σ_*, suggesting that their bulges are in this respect identical. Moreover, all NLS1s of our sample fall below the fit, showing σ_*-values higher than expected, and also below the relations found by Gebhardt et al. (2000a), Merritt & Ferrarese (2001) and Tremaine et al. (2002), which on the contrary are well in agreement with our S1s values. This discrepancy between the two results could be caused by the assumption of [O III] widths as representative of the stellar kinematics. Indeed, the [O III]-σ_* conversion has a large scatter and is not yet proved to be valid for NLS1 galaxies. Therefore, we stress the necessity to directly measure σ_*, for example observing NLS1s in spectral ranges different from the optical one.

Since both relations are based on important assumptions, which can introduce significant errors, at the moment it is not possible to favor one over the other. The fact that, according to our first results, NLS1 galaxies seem to have less massive bulges harboring equally less massive BHs than S1 galaxies, strongly indicates that the hypothesis of an inclination effect of a disklike BLR on the narrowness of Balmer emission lines should be rejected, at least for most NLS1s. A pure selection effect is not expected to be related to the physical properties of the bulges, and therefore NLS1s should be just those S1s with intrinsically smaller bulges to justify the difference we observe between NLS1s and S1s. On the other hand, our second result confirms the smaller $M_{\rm BH}/M_{\rm bulge}$ ratio in NLS1s, which led Mathur et al. (2001) and Grupe & Mathur (2004) to suggest an evolutionary scenario for these AGNs toward an S1 stage. In particular, NLS1s would be AGNs in a phase in which BHs are growing independently from their hosting environment.

However, both cases support the general idea of NLS1s in terms of AGNs with less massive BHs accreting matter at high rates in order to maintain nuclear luminosities comparable to those of S1s, as we said above. Moreover, our results are not in conflict with the evolutionary scenario and sustain the idea that NLS1s are likely to be young S1s, even in case of a joined evolution of BH and bulge. In fact, calculations by Bian & Zhao (2003) suggest timescales on the order of some $\sim 10^8$ yr for an NLS1 to become an S1. This timescale is in agreement with the growth time of a spiral bulge through minor merger phenomena. Indeed, Walker, Mihos, & Hernquist (1996) demonstrated through *N*-body simulations that a minor merger makes significant disturbances to the morphology of a larger galaxy in less than 1 Gyr from the onset of the merger. Moreover, Aguerri, Balcells, & Peletier (2001) showed that the accretion of small satellites is an effective mechanism for the growth of bulges in spiral galaxies.

We are grateful to the referee for valuable comments that improved the quality of the paper. V. B. is grateful to Y. Lu, S. Kaspi, and T. Boller for valuable suggestions. S. C. is grateful to S. Temporin for having supported this work with useful discussions. This research was partially based on data from the ING archive. In this work we have used the NASA/IPAC Extragalactic Database (NED), which is operated by the Jet Propulsion Laboratory, California Institute of Technology, under contract with the National Aeronautics and Space Administration. This research has made use of the TARTARUS database, which is supported by Jane Turner and Kirpal Nandra under NASA grants NAG 5-7385 and NAG 5-7067.

REFERENCES

Aguerri, J. A. L., Balcells, M., & Peletier, R. F. 2001, A&A, 367, 428
Barnes, J. E., & Hernquist, L. E. 1991, ApJ, 370, L65
Bian, W., & Zhao, Y. 2003, PASJ, 55, 143
———. 2004, MNRAS, 347, 607
Boller, T., Brandt, W. N., & Fink, H. 1996, A&A, 305, 53
Boroson, T. A., & Green, R. F. 1992, ApJS, 80, 109
Cardelli, J. A., Clayton, G. C., & Mathis, J. S. 1989, ApJ, 345, 245
Crenshaw, D. M., et al. 2002, ApJ, 566, 187
de Vaucouleurs, G., de Vaucouleurs, A., Corwin, H. G., Buta, R. J., Paturel, G., & Fouque, P. 1991, Third Reference Catalogue of Bright Galaxies (Berlin: Springer)
Ferrarese, L., & Merritt, D. 2000, ApJ, 539, L9
Gebhardt, K., et al. 2000a, ApJ, 539, L13
———. 2000b, ApJ, 543, L5
Granato, G. L., Zitelli, V., Bonoli, F., Danese, L., Bonoli, C., & Delpino, F. 1993, ApJS, 89, 35
Grupe, D., & Mathur, S. 2004, ApJ, 606, L41
Helou, G., Soifer, B. T., & Rowan-Robinson, M. 1985, ApJ, 298, L7
Ho, L. 1999, in Observational Evidence for the Black Holes in the Universe, ed. S. Chakrabarti (Dordrecht: Kluwer), 157
Kaspi, S., Smith, P. S., Netzer, H., Maoz, D., Jannuzi, B. T., & Giveon, U. 2000, ApJ, 533, 631
Komossa, S., & Mathur, S. 2001, A&A, 374, 914
Kormendy, J., & Richstone, D. 1995, ARA&A, 33, 581
Jahnke, K., & Wisotzki, L. 2003, MNRAS, 346, 304
Laor, A. 1998, ApJ, 505, L83
———. 2001, ApJ, 553, L667
Leighly, K. M. 1999, ApJS, 125, 317
MacKenty, J. W. 1990, ApJS, 72, 231
Magorrian, J., et al. 1998, AJ, 115, 2285
Malumyan, V. H., & Panajyan, V. G. 2000, Astrophysics, 43, 403
Marconi, A., & Hunt, L. K. 2003, ApJ, 589, L21
Mathur, S. 2000, MNRAS, 314, 17
Mathur, S., Kuraszkiewicz, J., & Czerny, B. 2001, NewA, 6, 321
McLure, R. J., & Dunlop, J. S. 2001, MNRAS, 327, 199
———. 2002, MNRAS, 331, 795

Merritt, D., & Ferrarese, L. 2001, ASP Conf. Ser. 249, The Central Kiloparsec of Starbursts and AGN: The La Palma Connection, ed. J. H. Knapen, J. E., Beckman, I. Shlosman, & T. J. Mahoney (San Francisco: ASP), 335
Nelson, C. H. 2000, ApJ, 544, L91
Nelson, C. H., & Whittle, M. 1995, ApJS, 99, 67
———. 1996, ApJ, 465, 96
Osterbrock, D. E. 1989, Astrophysics of Gaseous Nebulae and Active Galactic Nuclei (Mill Valley: University Science Books)
Osterbrock, D. E., & Pogge, R. W. 1985, ApJ, 297, 166
Padovani, P., & Rafanelli, P. 1988, A&A, 205, 53
Persson, S. E. 1988, ApJ, 330, 751
Peterson, B. M. 1993, PASP, 105, 247
Peterson, B. M., et al. 2000, ApJ, 542, 161
Peterson, B. M., & Wandel, A. 1999, ApJ, 521, L95
Pounds, K. A., Stanger, V. J., Turner, T. J., King, A. R., & Czerny, B. 1987, MNRAS, 224, 443
Prugniel, P., & Heraudeau, P. 1998, A&AS, 128, 299
Schlegel, D. J., Finkbeiner, D. P., & Davis, M. 1998, ApJ, 500, 525
Schmitt, H. R., & Kinney, A. R. 2000, ApJS, 128, 479
Simien, F., & de Vaucouleurs, G. 1986, ApJ, 302, 564
Smith, J. E., Young, S., Robinson, A., Corbett, E. A., Giannuzzo, M. E., Axon, D. J., & Hough, J. H. 2002, MNRAS, 335, 773
Strateva, I. V., Strauss, M. A., Hao, L., & Schlegel, D. J. 2003, AJ, 126, 1720
Tremaine, S., et al. 2002, ApJ, 574, 740
Véron-Cetty, M.-P., Véron, P., & Gonçalves, A. C. 2001, A&A, 372, 730
Vestergaard, M., Wilkes, B. J., & Barthel, P. D. 2000, ApJ, 538, L103
Walker, I. R., Mihos, J. C., & Hernquist, L. 1996, ApJ, 460, 121
Wandel, A. 1999, ApJ, 519, L39
———. 2002, ApJ, 565, 762
Wandel, A., Peterson, B. M., & Malkan, M. A. 1999, ApJ, 526, 579
Wang, T., & Lu, Y. 2001, A&A, 377, 52
Wang, Y. P., Biermann, P. L., & Wandel, A. 2000, A&A, 361, 550
Whittle, M. 1992, ApJS, 79, 49
Winkler, H. 1997, MNRAS, 292, 273
Wu, X.-B., & Han, J. L. 2001, A&A, 380, 31